Rare beauty and charm decays

Angel Campoverde on behalf of the LHCb Collaboration

EW Moriond, March 27th 2024

LHCb

中国科学院大学
University of Chinese Academy of Sciences

Introduction

Two ways to search for New Physics.

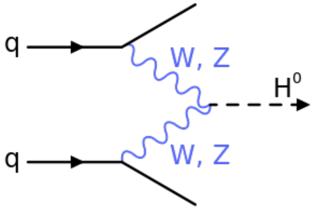

VBF

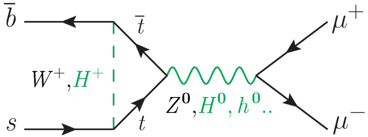

$B_s^0 \to \mu^+\mu^-$

- More sensitive to specific models
- **BUMP!** $\Rightarrow$ easier to interpret as NP
- Less prone to systematic effects
- Limited by LHC collision energy

- Sensitive to anything that is not SM.
- Rare decays $\Rightarrow$ more sensitive to NP.
- Use of ratios $\Rightarrow$ can cancel systematics.
- Less limited by LHC collision energy.

Outline

- Measurement of $\mathcal{B}(\phi \to \mu^+\mu^-)/\mathcal{B}(\phi \to e^+e^-)$.
  [LHCb-PAPER-2023-038]
- Search of $B_c \to \pi^+\mu^+\mu^-$ and measurement of $\mathcal{B}(B_c \to \psi(2S)\pi^+)/\mathcal{B}(B_c \to J/\psi\pi^+)$.
  [LHCb-PAPER-2023-037]
- Search for $B_s^0 \to \mu^+\mu^-\gamma$. [LHCb-PAPER-2023-045] in preparation
- Amplitude analysis $\Lambda_b^0 \to pK^-\gamma$. [LHCb-PAPER-2023-036] in preparation

Measurement of $\mathcal{B}(\phi \to \mu^+\mu^-)/\mathcal{B}(\phi \to e^+e^-)$

Decay allows us to understand efficiencies at low $q^2 \equiv m^2(\ell, \ell)$.
Data: 5.4fb^{-1}from 2016, 2017 and 2018.

$$R_{\phi\pi}^{(s)} = \beta_{\mu/e} \frac{\mathcal{B}(D_{(s)}^+ \to \pi^+\phi(\mu^+\mu^-))}{\mathcal{B}(D_{(s)}^+ \to \pi^+\phi(e^+e^-))} \Bigg/ \frac{\mathcal{B}(B^+ \to K^+ J/\psi(\mu^+\mu^-))}{\mathcal{B}(B^+ \to K^+ J/\psi(e^+e^-))}$$

Where $\beta_{\mu/e}$ is a phase space factor.

- **Low q^2:** Tracks with $p_T > 300$MeV/c and $p > 2000$MeV/c.
- **Triggered by:** Signal e, μ, π or object not associated to candidate.
- **Electron bremsstrahlung recovery:** Find photons by extrapolating electron track.

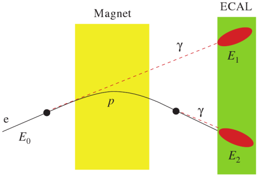

- **Kinematical constraints:** Unlike R_K or R_K^* , $m(\ell, \ell)$ is constrained also in signal channel ⇒ better resolution.

[LHCb-PAPER-2023-038]

Measurement of $\mathcal{B}(\phi \to \mu^+\mu^-)/\mathcal{B}(\phi \to e^+e^-)$

$D_s^+ \to \pi^+\phi(\to e^+e^-)$ backgrounds:

Misidentified:

- $D^+ \to K^+_{\to e^+}\pi^-_{\to e^-}\pi^+$: Removed by vetoing mass around D^+.
- $D^+ \to \pi^+_{\to e^+}\pi^-_{\to e^-}\pi^+$: Reduced with PID requirements, dominant

Combinatorial: *Warped* by constraint on $m(e^+, e^-)$ to be around $m(\phi)$

[LHCb-PAPER-2023-038]

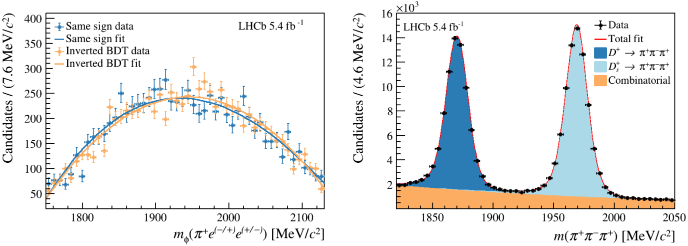

Validation of combinatorial and mis-ID backgrounds.

$B^+ \to K^+ J/\psi(\to \ell\ell)$ backgrounds:

- Partially reconstructed: $B^{0,+} \to K^+\pi^{-,0} J/\psi(\to e^+e^-)$
- Misidentified: $B^+ \to \pi^+ J/\psi(\to \ell\ell)$, small
- Combinatorial: Modelled with exponential.

Measurement of $\mathcal{B}(\phi \to \mu^+\mu^-)/\mathcal{B}(\phi \to e^+e^-)$

Muon

Electron

Signal

Normalization

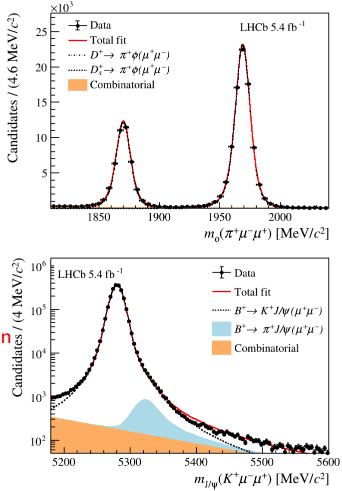

[LHCb-PAPER-2023-038]

Measurement of $\mathcal{B}(\phi \to \mu^+\mu^-)/\mathcal{B}(\phi \to e^+e^-)$

Main systematics:

- q^2 resolution: Normalization mode corrections do not port well to low q^2.
- Event multiplicity: Only partial cancellation with normalization mode.

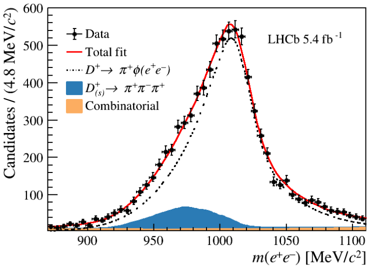

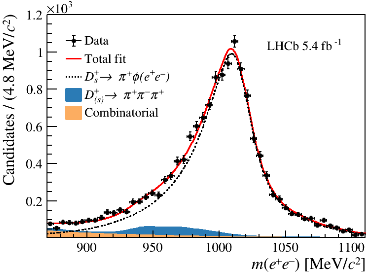

[LHCb-PAPER-2023-038]

Consistent between channels

$$R^d_{\phi\pi} = 1.026 \pm 0.020\,(\text{stat}) \pm 0.056\,(\text{syst}),$$
$$R^s_{\phi\pi} = 1.017 \pm 0.013\,(\text{stat}) \pm 0.051\,(\text{syst}).$$

Driven by systematics

$$\rightarrow R_{\phi\pi} = 1.022 \pm 0.012\,(\text{stat}) \pm 0.048\,(\text{syst}).$$

6% ⇒ <2%

$$\mathcal{B}(\phi \to \mu^+\mu^-) = (3.045 \pm 0.049\,(\text{stat}) \pm 0.148\,(\text{syst})) \times 10^{-4},$$

Angel F. Campoverde

$R_{\pi^+\mu^+\mu^-/J/\psi}$ and $R_{\psi(2S)/J/\psi}$

First search of non-resonant $B_c^+ \to \pi^+\mu^+\mu^-$, can be used to search for $B_c^+ \to B_{(s)}^{*0}\pi^+$.

[LHCb-PAPER-2023-037]

- **Data:** 9fb^{-1}, full LHCb dataset.
- **Strategy:**
  - Use $B_c^+ \to \pi^+ J/\psi(\to \mu^+\mu^-)$ as normalization and control channel to measure:

$$R_{\psi(2S)/J/\psi} \equiv \frac{\mathcal{B}(B_c^+ \to \psi(2S)\pi^+)}{\mathcal{B}(B_c^+ \to J\psi\pi^+)} \qquad R_{\pi^+\mu^+\mu^-/J/\psi} \equiv \frac{\mathcal{B}(B_c^+ \to \mu^+\mu^-\pi^+)}{\mathcal{B}(B_c^+ \to J\psi\pi^+)}$$

- Analysis done in bins of q^2 and constraining $m(\mu^+,\mu^-)$ to charmonium mass for measurement of $R_{\psi(2S)/J/\psi}$.

$B_c^+ \to J/\psi\pi^+$
$|m(\mu^+,\mu^-) - m_{J/\psi}| < 50$ MeV

$B_c^+ \to \psi(2S)\pi^+$
$|m(\mu^+,\mu^-) - m_{\psi(2S)}| < 50$ MeV

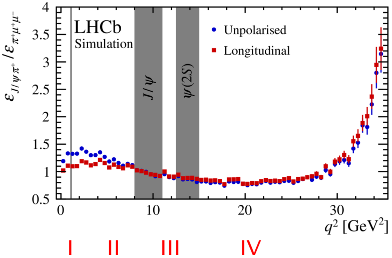

- Trigger on muons.

$R_{\pi^+\mu^+\mu^-/J/\psi}$ and $R_{\psi(2S)/J/\psi}$

Unconstrained

Non-resonant

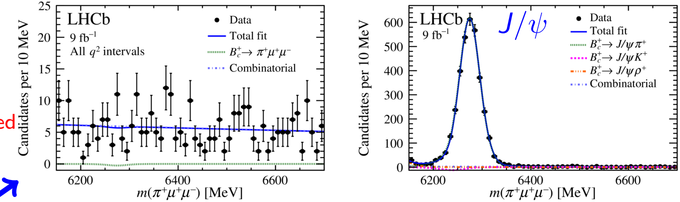

Fits for $R_{\pi^+\mu^+\mu^-/J/\psi}$

Different MVA cuts

Constrained

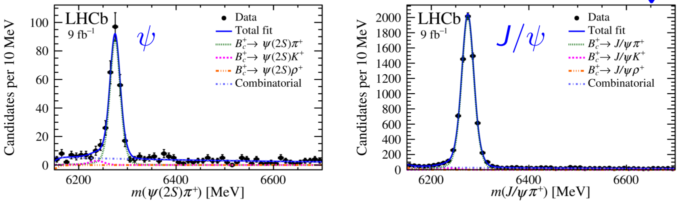

Fits for $R_{\psi(2S)/J/\psi}$

[LHCb-PAPER-2023-037]

Mass scales and resolutions:

- **Rare mode:** Constrained to value from $B_c^+ \to J/\psi\pi^+$ fits.
- **Resonant modes:** Floating but shared among components.

$R_{\pi^+\mu^+\mu^-/J/\psi}$ and $R_{\psi(2S)/J/\psi}$

No signal observed in non-resonant mode $\Rightarrow$ Set upper limits.

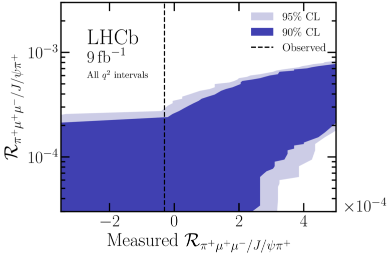

No theory predictions available

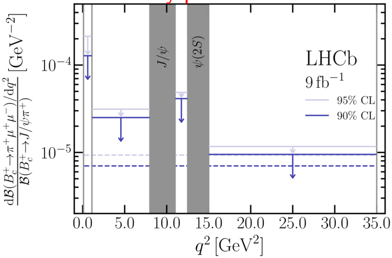

[LHCb-PAPER-2023-037]

First upper limit

$$\frac{\mathcal{B}(B_c^+ \to \pi^+\mu^+\mu^-)}{\mathcal{B}(B_c^+ \to J/\psi\pi^+)} < 2.1 \times 10^{-4}$$

$$\frac{\mathcal{B}(B_c^+ \to \psi(2S)\pi^+)}{\mathcal{B}(B_c^+ \to J/\psi\pi^+)} = 0.254 \pm 0.018\,(\text{stat}) \pm 0.003\,(\text{syst}) \pm 0.005\,(\text{BF})$$

Most precise to date

Search for the $B_s^0 \to \mu^+\mu^-\gamma$ decay

- Presence of photon lifts chiral suppression and sets its BR at the same order of magnitude as $B_s^0 \to \mu^+\mu^-$.
- Upper limit of $\mathcal{B}(B_s^0 \to \mu^+\mu^-\gamma) < 2 \cdot 10^{-9}$ set @ 95% CL by PhysRevD.105.012010

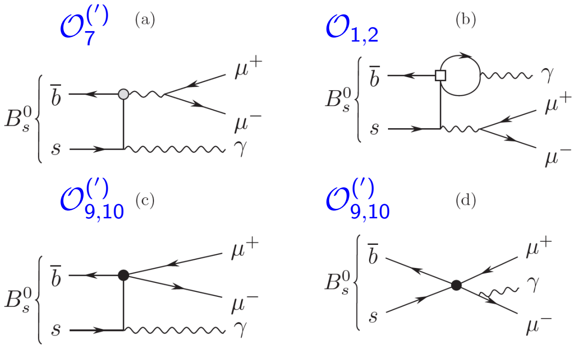

Sensitive to more operators than $B_s^0 \to \mu^+\mu^-$

[LHCb-PAPER-2023-045] in preparation

Search for the $B_s^0 \to \mu^+\mu^-\gamma$ decay

Measurement carried out in 4 bins in q^2 and studying low-q^2 bin with ϕ veto.

Control channel
$B_s \to \phi(\to K^+K^-)\gamma$
Large statistics

Normalization channel
$B_s \to J/\psi(\to \mu\mu)\eta$
$\eta \to \gamma\gamma$
Well known $\mathcal{BR}$

Trigger on:
Muons and photon

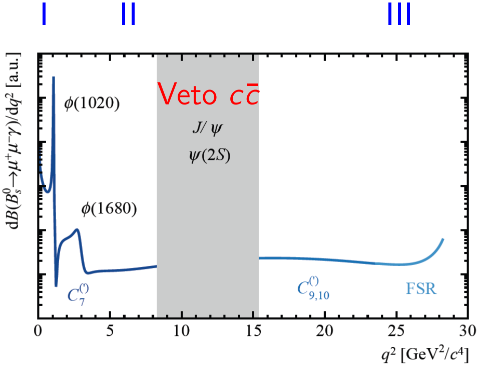

q^2 bin	I	II	III
q^2 [GeV$^2/c^4$]	$[4\,m_\mu^2, 2.89]$	$[2.89, 8.29]$	$[15.37, m_{B_s^0}^2]$
$m(\mu^+\mu^-)$ [GeV$/c^2$]	$[2\,m_\mu, 1.70]$	$[1.70, 2.88]$	$[3.92, m_{B_s^0}]$
$10^{10} \times \mathcal{B}(B_s^0 \to \mu^+\mu^-\gamma)$ [8]	82 ± 15	2.54 ± 0.34	9.1 ± 1.1
Fraction of $B_s^0 \to \mu^+\mu^-\gamma$	87%	2.7%	9.8%

[LHCb-PAPER-2023-045] in preparation

Search for the $B_s^0 \to \mu^+\mu^-\gamma$ decay

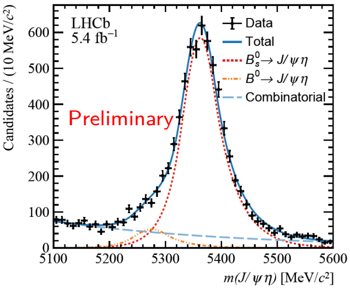

Normalization

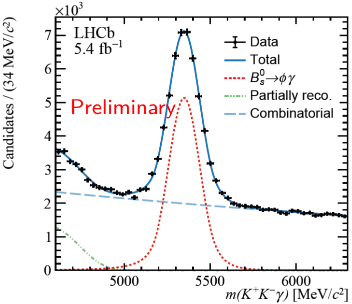

Control

[LHCb-PAPER-2023-045] in preparation

Normalization: Used to extract $\mathcal{B}(B_s^0 \to \mu^+\mu^-\gamma)$

$$\mathcal{B}(B_s^0 \to \mu^+\mu^-\gamma) = \frac{\mathcal{B}_{\rm norm}}{N_{\rm norm}} \times f_{\rm norm} \times N_{\rm sig}$$

Control: Used to calibrate efficiencies.

$$f_{\rm norm} = \frac{\epsilon^{\rm Acceptance}_{\rm norm}}{\epsilon^{\rm Acceptance}_{\rm sig}} \times \frac{\epsilon^{\rm Preselection}_{\rm norm}}{\epsilon^{\rm Preselection}_{\rm sig}} \times \frac{\epsilon^{\rm PID}_{\rm norm}}{\epsilon^{\rm PID}_{\rm sig}} \times \frac{\epsilon^{\rm Trigger}_{\rm norm}}{\epsilon^{\rm Trigger}_{\rm sig}} \times \frac{\epsilon^{\rm MLP}_{\rm norm}}{\epsilon^{\rm MLP}_{\rm sig}}$$

$$f^{\rm bin\ I}_{\rm norm} = 0.85 \pm 0.07,$$
$$f^{\rm bin\ II}_{\rm norm} = 0.95 \pm 0.08,$$
$$f^{\rm bin\ III}_{\rm norm} = 2.20 \pm 0.07,$$

Angel F. Campoverde

Search for the $B_s^0 \to \mu^+\mu^-\gamma$ decay

No excess $\Rightarrow$ set upper limits

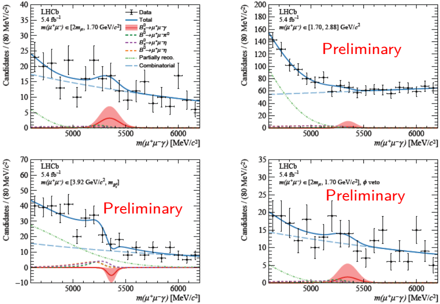

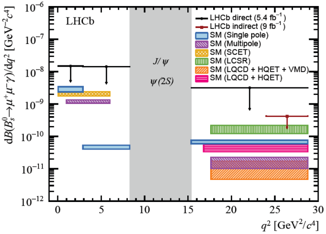

[LHCb-PAPER-2023-045] in preparation

$$\mathcal{B}(B_s^0 \to \mu^+\mu^-\gamma)_{\rm I} < 3.6\,(4.2) \times 10^{-8},$$
$$\mathcal{B}(B_s^0 \to \mu^+\mu^-\gamma)_{\rm II} < 6.5\,(7.7) \times 10^{-8},$$
$$\mathcal{B}(B_s^0 \to \mu^+\mu^-\gamma)_{\rm III} < 3.4\,(4.2) \times 10^{-8},$$

Dominated by statistical uncertainty

$$\mathcal{B}(B_s^0 \to \mu^+\mu^-\gamma)_{\rm I,\ with\ \phi\ veto} < 2.9\,(3.4) \times 10^{-8},$$
$$\mathcal{B}(B_s^0 \to \mu^+\mu^-\gamma)_{\rm comb.} < 2.5\,(2.8) \times 10^{-8},$$

Amplitude analysis of the $\Lambda_b^0 \to pK^-\gamma$ decay

- **Data:** 9fb^{-1}, entire LHCb dataset.
- Theory predictions only available for decays through $\Lambda(1520)$
- Complementary analysis to $\Lambda_b^0 \to pK^- J/\psi$ that can access pK^- masses up to 2.5GeV.

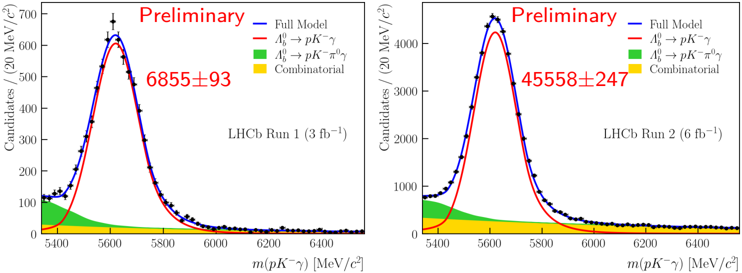

Selection ⇒ mass fit ⇒ background subtraction ⇒ Amplitude analysis

[LHCb-PAPER-2023-036] in preparation

Backgrounds:

- **Combinatorial:** Reduced with MVA using kinematic quantities and isolation
- **Mis-ID:** Found to be negligible.
- **Partially reconstructed:** Modelled.

Amplitude analysis of the $\Lambda_b^0 \to pK^-\gamma$ decay

Photon resolution worsens Dalitz plane resolution $\Rightarrow$ Apply mass constraint on Λ_b^0 fit to get $m_{\Lambda_b^0}(p\gamma)$ and $m_{\Lambda_b^0}(pK)$

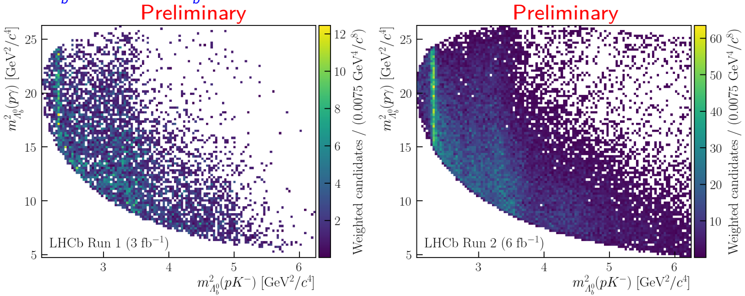

Model of amplitude taken from JHEP06(2020)116

$$\mathrm{NLL} \equiv -\log(\mathcal{L}) = -\sum_{\mathrm{Run\ 1}} \log\left(f_1\left(\mathcal{D}\right)\right) w_s - \sum_{\mathrm{Run\ 2}} \log\left(f_2\left(\mathcal{D}\right)\right) w_s$$

Parameter of Interest: Couplings between Λ_b^0 and daughter Λ resonances.

- w_s: sPlot weights used to background subtract.
- $\mathcal{D}$: 2 coordinates in Dalitz plane.

[LHCb-PAPER-2023-036] in preparation

Amplitude analysis of the $\Lambda_b^0 \to pK^-\gamma$ decay

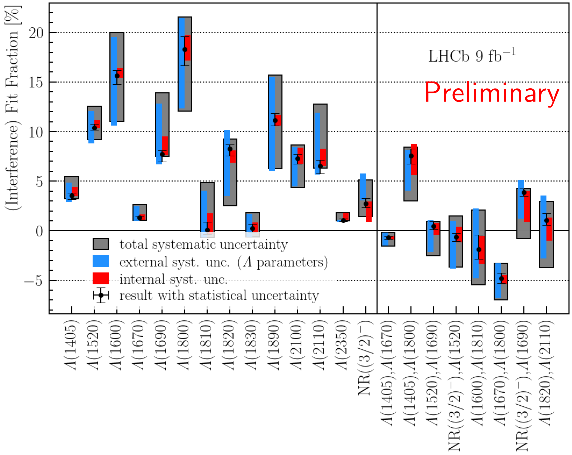

[LHCb-PAPER-2023-036] in preparation

Systematics:

- **Leading:** Lineshapes of Λ resonances (external)
- **Subleading:** Amplitude model, acceptance, sample size, mass fits, etc (internal)

Summary

- Rare B meson decays offer an alternative way to search for new physics.
- The first two analyses shown have provided:
  - A measurement of $R_{\phi\pi}^{(d,s)}$ and the most precise measurement of $\mathcal{B}(\phi \to \mu^+\mu^-)$.
  - The most precise measurement of $R_{\psi(2S)/J/\psi}$ and the first upper limit for the non-resonant mode $B_c^+ \to \pi^+\mu^+\mu^-$.
- The other two have confirmed and strengthened upper bounds on $\mathcal{B}(B_s^0 \to \mu^+\mu^-\gamma)$ and explored decays of Λ_b not well known.
- LHCb will start collecting data again this year with its software only trigger.
- Many results will be updated and we expect tighter constrains, specially for the statistically limited measurements.

Backup

Measurement of $\mathcal{B}(\phi \to \mu^+\mu^-)/\mathcal{B}(\phi \to e^+e^-)$

Both signal and normalization mode use maximum likelihood fits with constraints on the dilepton mass

Channel	$\phi(1020)$ [MeV/c^2]	J/ψ [MeV/c^2]
Electrons	870-1110	2450-3600
Muons	990-1050	2946-3176

Table: Mass cuts for ϕ and J/ψ.

Decay mode	$m_\phi(\pi^+\ell^+\ell^-)$ [MeV/c^2]	$m_{J/\psi}(K^+\ell^+\ell^-)$ [MeV/c^2]
e^+e^-	$\notin$ [1810,2040]	> 5580
$\mu^+\mu^-$	$\notin$ [1840,2000]	> 5480

Decay mode	Yield
$D^+ \to \pi^+\phi(\to e^+e^-)$	$7\,460 \pm 140$
$D^+ \to \pi^+\phi(\to \mu^+\mu^-)$	$43\,512 \pm 220$
$D_s^+ \to \pi^+\phi(\to e^+e^-)$	$16\,740 \pm 210$
$D_s^+ \to \pi^+\phi(\to \mu^+\mu^-)$	$87\,022 \pm 300$
$B^+ \to K^+J/\psi(\to e^+e^-)$	$638\,600 \pm 900$
$B^+ \to K^+J/\psi(\to \mu^+\mu^-)$	$2\,187\,000 \pm 1\,500$

Figure: Mass ranges for mass sidebands and fit yields

Measurement of $\mathcal{B}(\phi \to \mu^+\mu^-)/\mathcal{B}(\phi \to e^+e^-)$

Data driven corrections are applied to simulation before extracting efficiencies.

- Quark kinematics
- Particle identification
- Trigger efficiencies
- Tracking efficiency
- q^2 resolution.

Total efficiency is obtained by:

- Adding between trigger categories.
- Performing luminosity weighted average between run periods.

Total yield is sum of yields from each run period fit. They are then put together in:

$$R_{\phi\pi}^{(d,s)} = \frac{N^{(d,s)}(\pi^+\phi(\to \mu^+\mu^-))}{N^{(d,s)}(\pi^+\phi(\to e^+e^-))} \frac{\varepsilon^{(d,s)}(\pi^+\phi(\to e^+e^-))}{\varepsilon^{(d,s)}(\pi^+\phi(\to \mu^+\mu^-))} \Big/ r_{J/\psi}$$

Can also be written as:

$$R_{\phi\pi}^{(s)} = \beta_{\mu/e} \frac{\mathcal{B}(D_{(s)}^+ \to \pi^+\phi(\mu^+\mu^-))}{\mathcal{B}(D_{(s)}^+ \to \pi^+\phi(e^+e^-))} \Bigg/ \frac{\mathcal{B}(B^+ \to K^+J/\psi(\mu^+\mu^-))}{\mathcal{B}(B^+ \to K^+J/\psi(e^+e^-))}$$

Measurement of $\mathcal{B}(\phi \to \mu^+\mu^-)/\mathcal{B}(\phi \to e^+e^-)$

To correct mismodelling due to q^2 differences, smearing factors are measured in $B^+ \to K^+ J/\psi(\to e^+e^-)$ in data.

Signal MC is smeared and shape is used to fit $m(e, e)$ in signal events:

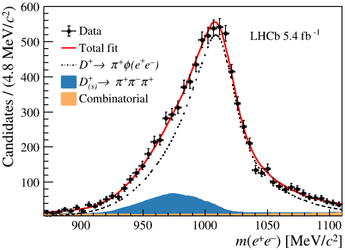

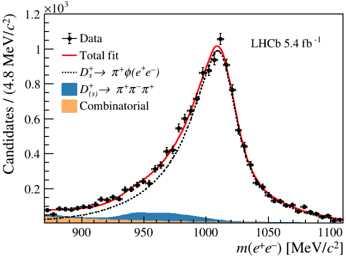

Fit quality validates smearing

Measurement of $\mathcal{B}(\phi \to \mu^+\mu^-)/\mathcal{B}(\phi \to e^+e^-)$

No significant trend is seen when $R_{\phi\pi}^{(0,s)}$ is measured in function of different variables.

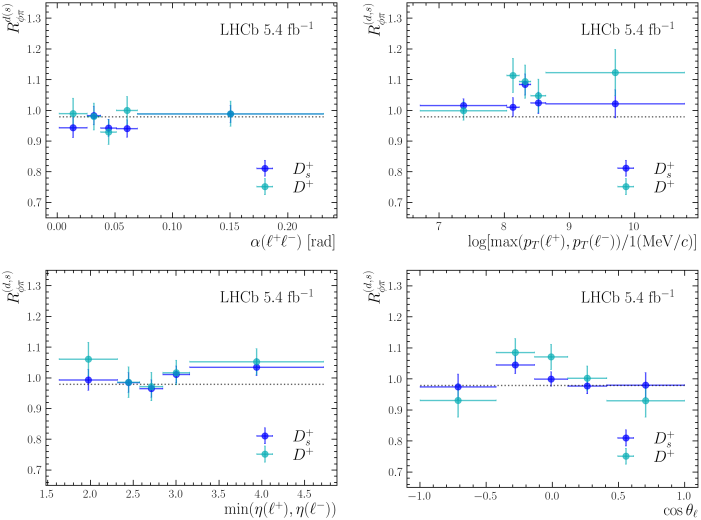

Measurement of $\mathcal{B}(\phi \to \mu^+\mu^-)/\mathcal{B}(\phi \to e^+e^-)$

Source	$R^d_{\phi\pi}$ [%]	$R^s_{\phi\pi}$ [%]
Resolution on q^2	4.0	3.9
Event multiplicity	2.7	2.7
Simulation reweighting	1.5	1.2
Combinatorial background shape parametrisation	1.5	1.0
PID	0.8	0.8
Finite size of control samples	0.8	0.6
Trigger	0.3	0.3
Tracking	0.1	0.1
Background from doubly misidentified electrons	1.1	0.1
Total	5.5	5.1

$R_{\pi^+\mu^+\mu^-/J/\psi}$ and $R_{\psi(2S)/J/\psi}$

Component	$\pi^+\mu^+\mu^-$ WP	$\psi(2S)\pi^+$ WP
$B_c^+ \to J/\psi\pi^+$	3508 ± 82	6887 ± 93
$B_c^+ \to J/\psi K^+$	-81 ± 58	90 ± 43
$B_c^+ \to J/\psi\rho^+$	41 ± 11	56 ± 22
Comb. bkg.	101 ± 25	1254 ± 60

(a) J/ψ yields

Component	Yield
$B_c^+ \to \psi(2S)\pi^+$	256 ± 18
$B_c^+ \to \psi(2S)K^+$	13 ± 10
$B_c^+ \to \psi(2S)\rho^+$	-4 ± 5
Comb. bkg.	197 ± 19

(b) $\psi(2S)$ yields

Simulation corrected for:

- Particle identification
- Track reconstruction efficiency.
- Trigger efficiency.
- B_c^+ lifetime, kinematics.
- Track multiplicity.

q^2 interval	$N_{\pi^+\mu^+\mu^-}$	N_{comb}
$0.1 < q^2 < 1.1\,\text{GeV}^2$	0 ± 2	$25\,^{+6}_{-5}$
$1.1 < q^2 < 8.0\,\text{GeV}^2$	$1\,^{+4}_{-3}$	39 ± 7
$11.0 < q^2 < 12.5\,\text{GeV}^2$	$-18\,^{+7}_{-10}$	$30\,^{+13}_{-9}$
$15.0 < q^2 < 35.0\,\text{GeV}^2$	$0\,^{+8}_{-7}$	232 ± 17
All	$-2\,^{+9}_{-8}$	$311\,^{+20}_{-19}$

(a) Rare mode yields

$R_{\pi^+\mu^+\mu^-/J/\psi}$ and $R_{\psi(2S)/J/\psi}$

Mass scales are shared between

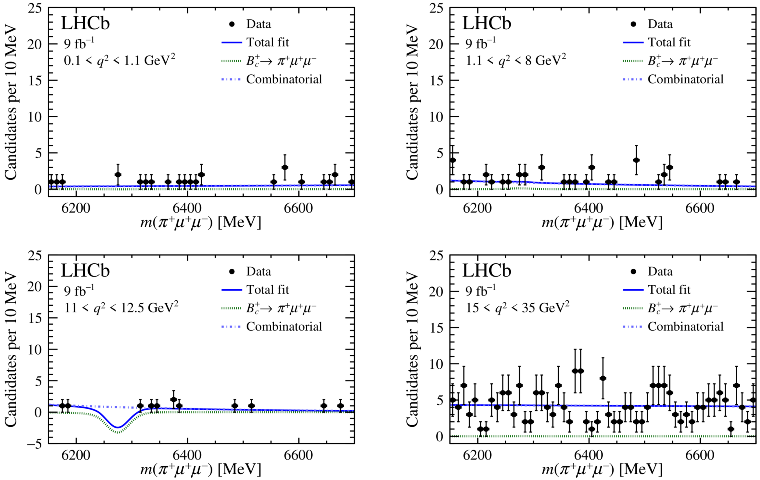

$R_{\pi^+\mu^+\mu^-/J/\psi}$ and $R_{\psi(2S)/J/\psi}$

Backgrounds:

- **Partially reco:** $B_c^+ \to \rho\mu^+\mu^-$, $B_c^+ \to J/\psi\rho^+$ and $B_c^+ \to \psi(2S)\rho^+$ with $\rho \to \pi^+\pi^0$. Included only for resonant fits .
- **Single Mis-ID:** Decays with Kaons reconstructed as pions in final state are Cabibbo suppresed and further suppressed by particle ID requirements .
- **Double Mis-ID:** E.g. $B_c^+ \to \pi^+\pi^-\pi^+$ or $B_c^+ \to c\bar{c}(\to \mu^+_{\to\pi^+}, \mu^-)\pi^+_{\to\mu^+}$ are suppressed by particle ID .

Selection uses BDT

- **Signal:** Simulated $B_c^+ \to \pi^+\mu^+\mu^-$, $B_c^+ \to \pi^+J/\psi(\to \mu^+\mu^-)$, $B_c^+ \to \pi^+B^{*0}(\to \mu^+\mu^-)$ and $B_c^+ \to \pi^+B_s^{*0}(\to \mu^+\mu^-)$
- **Background:** Data sidebands in $m(\pi^+\mu^+\mu^-)$, excluding charmonium from $m(\mu^+\mu^-)$ distribution.

MVA optimization FOM is different for each measurement

- $R_{\pi^+\mu^+\mu^-/J/\psi} \Rightarrow \varepsilon/(5/2 + \sqrt{N_B})$
- $R_{\psi(2S)/J/\psi} \Rightarrow N_S/\sqrt{N_S + N_B}$

Search for the $B_s^0 \to \mu^+\mu^-\gamma$ decay

Photons:

- $p_T > 1000$ MeV
- MVA based photon identification.
- For $p_T > 2000$ MeV MVA to separate them from merged photons in $\pi^0 \to \gamma\gamma$

Muons:

- $p_T > 250$ MeV
- Good quality and particle identification requirements

B_s

- $p_T > 500$ MeV
- Good vertex quality

Search for the $B_s^0 \to \mu^+\mu^-\gamma$ decay

Differences with respect to $B_s^0 \to \mu^+\mu^- \to$ PhysRevD.105.012010

$B_s^0 \to \mu^+\mu^-\gamma$

- This reconstructs the photon.
- Mesures $B_s^0 \to \mu^+\mu^-\gamma$ as signal
- Thanks to the photon can explore also lower regions in q^2

$B_s^0 \to \mu^+\mu^-$

- Reconstructs only the muons
- Measures $B_s^0 \to \mu^+\mu^-\gamma$ as part of the partially reconstructed background
- Can only have access to high q^2 regions $> 4.9\text{GeV}^2$

Both have set upper limits.

Search for the $B_s^0 \to \mu^+\mu^-\gamma$ decay

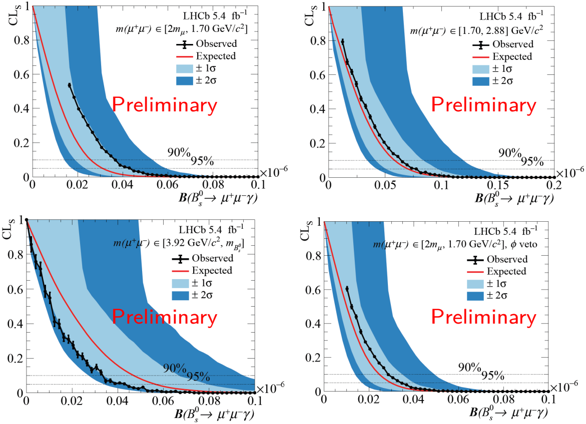

$$
\begin{aligned}
\mathcal{B}(B_s^0 \to \mu^+\mu^-\gamma)_{\text{bin I}} &= (1.34 \pm 1.60 \pm 0.28) \times 10^{-8}, \\
\mathcal{B}(B_s^0 \to \mu^+\mu^-\gamma)_{\text{bin II}} &= (0.76 \pm 3.55 \pm 0.30) \times 10^{-8}, \\
\mathcal{B}(B_s^0 \to \mu^+\mu^-\gamma)_{\text{bin III}} &= (-2.55 \pm 2.25 \pm 0.41) \times 10^{-8}, \\
\mathcal{B}(B_s^0 \to \mu^+\mu^-\gamma)_{\text{bin I}\ \phi\ \text{veto}} &= (0.72 \pm 1.56 \pm 0.29) \times 10^{-8}.
\end{aligned}
$$

Amplitude analysis of the $\Lambda_b^0 \to pK^-\gamma$ decay

Preselection:

- Λ_b^0: Good vertex quality, momentum pointing to PV
- p, K^-: $IP > 0.1mm$, $p_T > 1$GeV, $p > 5$GeV.
- γ: $E_T > 3$GeV

MVA:

- Uses kinematic variables and isolation
- **Background:** Upper sideband in data $m(pK\gamma) > m(\Lambda_b^0) + 300$MeV
- **FOM:** $S/\sqrt{S+B}$

$$I_{p_{\mathrm{T}}} = \frac{p_{\mathrm{T}}(\Lambda_b^0) - \sum p_{\mathrm{T}}}{p_{\mathrm{T}}(\Lambda_b^0) + \sum p_{\mathrm{T}}}$$

Amplitude analysis of the $\Lambda_b^0 \to pK^-\gamma$ decay

Mis-ID backgrounds:

- $B_s^0 \to \phi(\to KK)\gamma$: Veto $m(p_{\to K}, K)$ mass around m_ϕ.
- $B_s^0 \to KK\gamma$, $B_d \to K\pi\gamma$: Less than 0.5%.
- $\Lambda_b^0 \to pK\eta$, $\Lambda_b^0 \to pK\pi^0$: Less than 1-2%, limited by staying below 2.5GeVin $m(p, K)$.
- $\Xi_b^0 \to pK\gamma$: Negligible

Mis-ID and Combinatorial:

- $D^0 \to KK$ **and** $D^0 \to K\pi$ **combined with random** γ**:** Veto distorts signal acceptance $\Rightarrow$ included in fit.

Partially reconstructed:

- $\Lambda_b^0 \to pK^{*-}(\to K^-\pi 0)\gamma$ Included in fit.

Amplitude analysis of the $\Lambda_b^0 \to pK^-\gamma$ decay

Maximum likelihood fit uses:

- **Reduced model:** Well-established resonances and interferences.
- **Non resonant:** Seen to improve fit quality

Projections of 2D fit on $m_{\Lambda_b}(pK^-)$

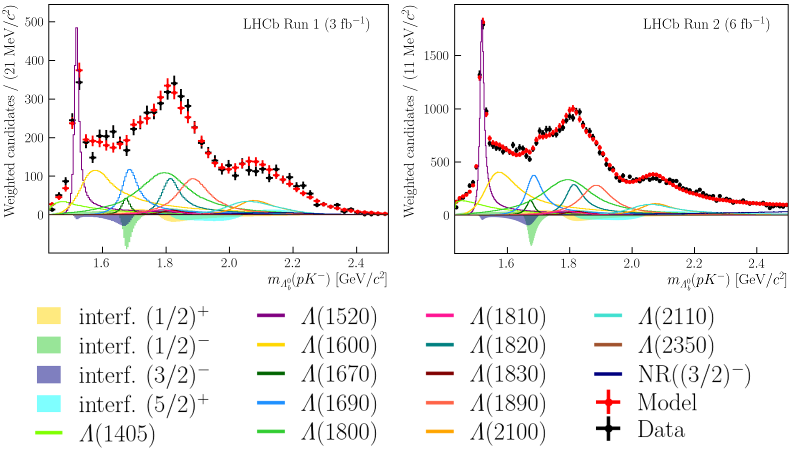

Amplitude analysis of the $\Lambda_b^0 \to pK^-\gamma$ decay

Mass fits:

- **Combinatorial:** Exponential
- **Signal:** Double sided Crystall Ball, tails from simulation
- **Partially reconstructed:** From Kernel density estimation on simulated $\Lambda_b^0 \to pK^{*-}(\to K^-\pi 0)\gamma$.

Amplitude analysis of the $\Lambda_b^0 \to pK^-\gamma$ decay

Resonance	J^P	m_0	Γ_0	Δm_0	$\Delta\Gamma_0$	σ_{m_0}	σ_{Γ_0}	l	L
$\Lambda(1405)$	$1/2^-$	1405	50.5	± 1.3	± 2	1.3	2	0	0, 1
$\Lambda(1520)$	$3/2^-$	1519	16	1518 – 1520	15 – 17	1	1	2	0, 1, 2
$\Lambda(1600)$	$1/2^+$	1600	200	1570 – 1630	150 – 250	30	50	1	0, 1
$\Lambda(1670)$	$1/2^-$	1674	30	1670 – 1678	25 – 35	4	5	0	0, 1
$\Lambda(1690)$	$3/2^-$	1690	70	1685 – 1695	50 – 70	5	10	2	0, 1, 2
$\Lambda(1800)$	$1/2^-$	1800	200	1750 – 1850	150 – 250	50	50	0	0, 1
$\Lambda(1810)$	$1/2^+$	1790	110	1740 – 1840	50 – 170	50	60	1	0, 1
$\Lambda(1820)$	$5/2^+$	1820	80	1815 – 1825	70 – 90	5	10	3	1, 2, 3
$\Lambda(1830)$	$5/2^-$	1825	90	1820 – 1830	60 – 120	5	30	2	1, 2, 3
$\Lambda(1890)$	$3/2^+$	1890	120	1870 – 1910	80 – 160	20	40	1	0, 1, 2
$\Lambda(2100)$	$7/2^-$	2100	200	2090 – 2110	100 – 250	10	100	4	2, 3, 4
$\Lambda(2110)$	$5/2^+$	2090	250	2050 – 2130	200 – 300	40	50	3	1, 2, 3
$\Lambda(2350)$	$9/2^+$	2350	150	2340 – 2370	100 – 250	20	100	5	3, 4, 5

Amplitude analysis of the $\Lambda_b^0 \to pK^-\gamma$ decay

Amplitude fit contains many parameters $\Rightarrow$ unstable.

- **Local minima:**
  - Fit ten times with different starting points.
  - Pick fit with lowest NLL.
- **Parameter variations:** Couplings vary between minima, but same values for
  - Fit fractions
  - Interference amplitudes

$\Rightarrow$ treat couplings as nuisance parameters and fit fractions and interference amplitudes as parameters of interest.

Amplitude analysis of the $\Lambda_b^0 \to pK^-\gamma$ decay

Resonances used in reduced model

Resonance	J^P	m_0	Γ_0	Δm_0	$\Delta\Gamma_0$	σ_{m_0}	σ_{Γ_0}	l	L
$\Lambda(1405)$	$1/2^-$	1405	50.5	± 1.3	± 2	1.3	2	0	0, 1
$\Lambda(1520)$	$3/2^-$	1519	16	1518 – 1520	15 – 17	1	1	2	0, 1, 2
$\Lambda(1600)$	$1/2^+$	1600	200	1570 – 1630	150 – 250	30	50	1	0, 1
$\Lambda(1670)$	$1/2^-$	1674	30	1670 – 1678	25 – 35	4	5	0	0, 1
$\Lambda(1690)$	$3/2^-$	1690	70	1685 – 1695	50 – 70	5	10	2	0, 1, 2
$\Lambda(1800)$	$1/2^-$	1800	200	1750 – 1850	150 – 250	50	50	0	0, 1
$\Lambda(1810)$	$1/2^+$	1790	110	1740 – 1840	50 – 170	50	60	1	0, 1
$\Lambda(1820)$	$5/2^+$	1820	80	1815 – 1825	70 – 90	5	10	3	1, 2, 3
$\Lambda(1830)$	$5/2^-$	1825	90	1820 – 1830	60 – 120	5	30	2	1, 2, 3
$\Lambda(1890)$	$3/2^+$	1890	120	1870 – 1910	80 – 160	20	40	1	0, 1, 2
$\Lambda(2100)$	$7/2^-$	2100	200	2090 – 2110	100 – 250	10	100	4	2, 3, 4
$\Lambda(2110)$	$5/2^+$	2090	250	2050 – 2130	200 – 300	40	50	3	1, 2, 3
$\Lambda(2350)$	$9/2^+$	2350	150	2340 – 2370	100 – 250	20	100	5	3, 4, 5

Amplitude analysis of the $\Lambda_b^0 \to pK^-\gamma$ decay

Reduced model (only resonances)

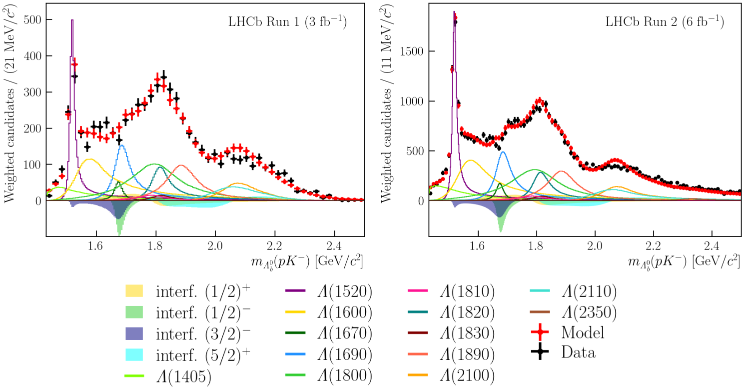

Amplitude analysis of the $\Lambda_b^0 \to pK^-\gamma$ decay

Reduced model plus non-resonant components

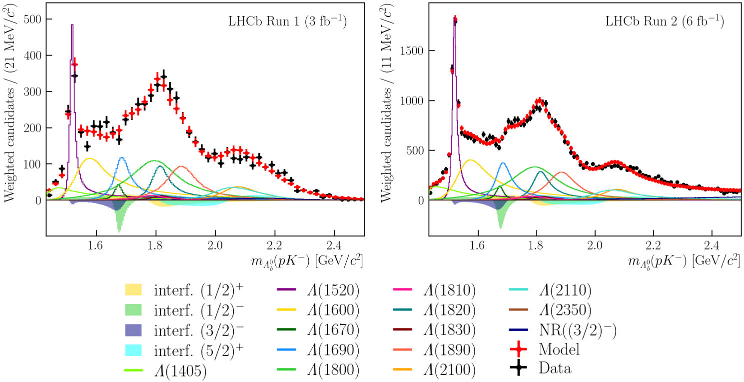

Amplitude analysis of the $\Lambda_b^0 \to pK^-\gamma$ decay

Reduced model (resonances and interferences) fit plus non-resonant (constant) components

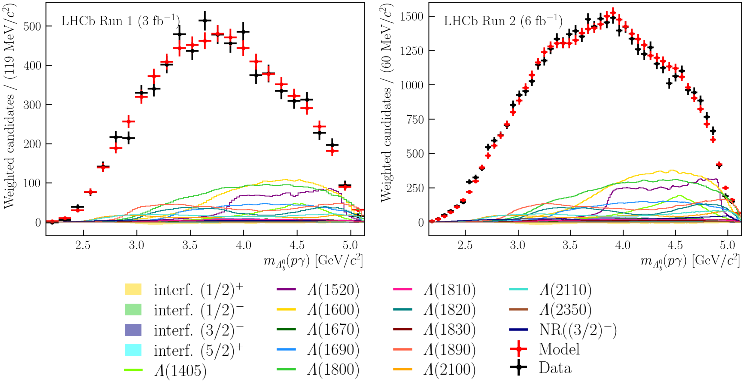

Amplitude analysis of the $\Lambda_b^0 \to pK^-\gamma$ decay

Reduced model (resonances and interferences) fit plus non-resonant (constant) components

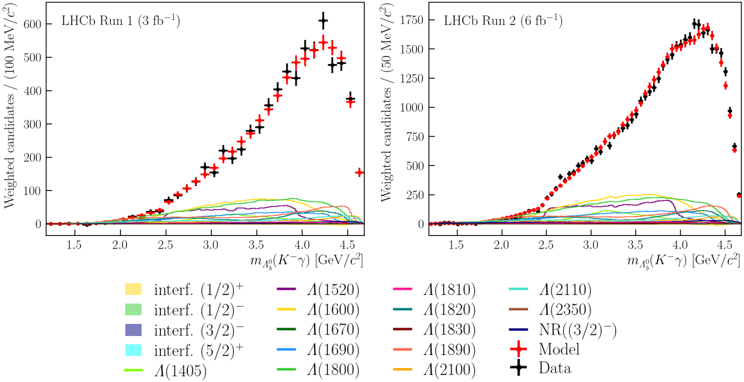

Amplitude analysis of the $\Lambda_b^0 \to pK^-\gamma$ decay

Systematics on fit fractions.

Observable	Amplitude model				Acceptance model			Mass fit model		
	$\sigma^{\Lambda}_{\text{BW}}$	$\sigma^{\Lambda}_{\text{radius}}$	$\sigma_{\text{amp.}}$	$\sigma_{\text{res.}}$	σ_{finite}	$\sigma_{\text{acc.}}$	$\sigma_{\text{kin.}}$	σ_{pK}	$\sigma_{p\gamma}$	$\sigma_{\text{comb.}}$
$\Lambda(1405)$	$^{+1.2}_{-0.7}$	$^{+0.0}_{-0.0}$	$^{+0.9}_{+0.2}$	$^{+0.0}_{-0.4}$	$^{+0.2}_{-0.2}$	$^{+0.2}_{-0.2}$	$^{+0.0}_{-0.0}$	$^{+0.0}_{-0.1}$	$^{+0.1}_{-0.0}$	$^{+0.0}_{-0.0}$
$\Lambda(1520)$	$^{+1.0}_{-1.3}$	$^{+1.1}_{-1.1}$	$^{+0.3}_{+0.0}$	$^{+0.0}_{-0.1}$	$^{+0.2}_{-0.2}$	$^{+0.2}_{-0.2}$	$^{+0.1}_{-0.1}$	$^{+0.3}_{-0.0}$	$^{+0.1}_{-0.0}$	$^{+0.0}_{-0.1}$
$\Lambda(1600)$	$^{+3.6}_{-4.5}$	$^{+1.8}_{-1.8}$	$^{+0.5}_{+0.0}$	$^{+0.3}_{-0.2}$	$^{+0.3}_{-0.3}$	$^{+0.2}_{-0.2}$	$^{+0.1}_{-0.1}$	$^{+0.0}_{-0.1}$	$^{+0.1}_{-0.0}$	$^{+0.0}_{-0.0}$
$\Lambda(1670)$	$^{+1.1}_{-0.3}$	$^{+0.2}_{-0.2}$	$^{+0.2}_{-0.2}$	$^{+0.2}_{-0.2}$	$^{+0.1}_{-0.1}$	$^{+0.0}_{-0.0}$	$^{+0.0}_{-0.0}$	$^{+0.0}_{-0.0}$	$^{+0.0}_{-0.0}$	$^{+0.0}_{-0.0}$
$\Lambda(1690)$	$^{+4.1}_{-0.3}$	$^{+2.0}_{-2.0}$	$^{+1.5}_{+0.2}$	$^{+0.6}_{-0.5}$	$^{+0.2}_{-0.2}$	$^{+0.1}_{-0.1}$	$^{+0.0}_{-0.0}$	$^{+0.1}_{-0.0}$	$^{+0.0}_{-0.1}$	$^{+0.0}_{-0.0}$
$\Lambda(1800)$	$^{+3.0}_{-5.9}$	$^{+1.1}_{-1.1}$	$^{+0.1}_{-0.8}$	$^{+0.8}_{-1.5}$	$^{+0.3}_{-0.3}$	$^{+0.1}_{-0.1}$	$^{+0.1}_{-0.1}$	$^{+0.0}_{-0.0}$	$^{+0.6}_{-0.0}$	$^{+0.4}_{-0.0}$
$\Lambda(1810)$	$^{+3.7}_{-0.7}$	$^{+1.1}_{-1.1}$	$^{+1.5}_{+0.1}$	$^{+0.5}_{-1.4}$	$^{+0.2}_{-0.2}$	$^{+0.1}_{-0.1}$	$^{+0.0}_{-0.0}$	$^{+0.1}_{-0.0}$	$^{+0.2}_{-0.0}$	$^{+0.0}_{-0.0}$
$\Lambda(1820)$	$^{+1.8}_{-4.9}$	$^{+0.2}_{-0.2}$	$^{-0.0}_{-0.9}$	$^{+0.3}_{-0.4}$	$^{+0.3}_{-0.3}$	$^{+0.1}_{-0.1}$	$^{+0.0}_{-0.0}$	$^{+0.0}_{-0.3}$	$^{+0.1}_{-0.0}$	$^{+0.0}_{-0.1}$
$\Lambda(1830)$	$^{+1.3}_{-0.9}$	$^{+0.6}_{-0.6}$	$^{+0.3}_{-0.4}$	$^{+0.3}_{-0.5}$	$^{+0.1}_{-0.1}$	$^{+0.1}_{-0.1}$	$^{+0.0}_{-0.0}$	$^{+0.2}_{-0.0}$	$^{+0.1}_{-0.0}$	$^{+0.0}_{-0.0}$
$\Lambda(1890)$	$^{+4.2}_{-5.1}$	$^{+0.8}_{-0.8}$	$^{+0.4}_{-0.4}$	$^{+0.1}_{-0.4}$	$^{+0.2}_{-0.2}$	$^{+0.1}_{-0.1}$	$^{+0.0}_{-0.0}$	$^{+0.1}_{-0.0}$	$^{+0.1}_{-0.0}$	$^{+0.0}_{-0.0}$
$\Lambda(2100)$	$^{+1.0}_{-2.6}$	$^{+0.8}_{-0.8}$	$^{+0.9}_{-0.7}$	$^{+0.2}_{-0.2}$	$^{+0.1}_{-0.1}$	$^{+0.0}_{-0.0}$	$^{+0.0}_{-0.0}$	$^{+0.0}_{-0.0}$	$^{+0.1}_{-0.0}$	$^{+0.1}_{-0.0}$
$\Lambda(2110)$	$^{+5.0}_{-0.6}$	$^{+1.5}_{-1.5}$	$^{+1.5}_{-0.1}$	$^{+0.3}_{-0.2}$	$^{+0.1}_{-0.1}$	$^{+0.1}_{-0.1}$	$^{+0.0}_{-0.0}$	$^{+0.0}_{-0.2}$	$^{+0.0}_{-0.0}$	$^{+0.2}_{-0.0}$
$\Lambda(2350)$	$^{+0.0}_{-0.1}$	$^{+0.0}_{-0.0}$	$^{+0.6}_{-0.2}$	$^{+0.0}_{-0.0}$	$^{+0.0}_{-0.0}$	$^{+0.0}_{-0.0}$	$^{+0.0}_{-0.0}$	$^{+0.1}_{-0.0}$	$^{+0.1}_{-0.0}$	$^{+0.1}_{-0.0}$
$\text{NR}(\frac{3}{2}^-)$	$^{+2.9}_{+0.3}$	$^{+0.4}_{-0.4}$	$^{+1.0}_{-2.4}$	$^{+0.0}_{-0.6}$	$^{+0.1}_{-0.1}$	$^{+0.1}_{-0.1}$	$^{+0.0}_{-0.0}$	$^{+0.0}_{-0.1}$	$^{+0.0}_{-0.3}$	$^{+0.0}_{-0.0}$
$\Lambda(1405), \Lambda(1670)$	$^{+0.4}_{-0.7}$	$^{+0.3}_{-0.3}$	$^{+0.2}_{-0.0}$	$^{+0.1}_{-0.1}$	$^{+0.1}_{-0.1}$	$^{+0.0}_{-0.0}$	$^{+0.0}_{-0.0}$	$^{+0.0}_{-0.0}$	$^{+0.0}_{-0.0}$	$^{+0.0}_{-0.1}$
$\Lambda(1405), \Lambda(1800)$	$^{+0.5}_{-3.6}$	$^{+0.3}_{-0.3}$	$^{+0.1}_{-1.9}$	$^{+1.7}_{-0.4}$	$^{+0.2}_{-0.2}$	$^{+0.2}_{-0.2}$	$^{+0.0}_{-0.0}$	$^{+0.0}_{-0.0}$	$^{+0.0}_{-0.3}$	$^{+0.1}_{-0.0}$
$\Lambda(1520), \Lambda(1690)$	$^{+0.3}_{-2.3}$	$^{+0.9}_{-0.9}$	$^{-0.1}_{-0.7}$	$^{+0.5}_{-0.4}$	$^{+0.1}_{-0.1}$	$^{+0.0}_{-0.0}$	$^{+0.0}_{-0.0}$	$^{+0.0}_{-0.1}$	$^{+0.0}_{-0.0}$	$^{+0.0}_{-0.0}$
$\Lambda(1520), \text{NR}(\frac{3}{2}^-)$	$^{+1.2}_{-2.4}$	$^{+1.5}_{-1.5}$	$^{+0.5}_{-0.5}$	$^{+0.8}_{-0.4}$	$^{+0.1}_{-0.1}$	$^{+0.1}_{-0.1}$	$^{+0.0}_{-0.0}$	$^{+0.0}_{-0.0}$	$^{+0.0}_{-0.1}$	$^{+0.0}_{-0.0}$
$\Lambda(1600), \Lambda(1810)$	$^{+4.1}_{-2.8}$	$^{+0.6}_{-0.6}$	$^{+1.5}_{-0.7}$	$^{+0.9}_{-0.4}$	$^{+0.3}_{-0.3}$	$^{+0.2}_{-0.2}$	$^{+0.0}_{-0.0}$	$^{+0.0}_{-0.0}$	$^{+0.0}_{-0.4}$	$^{+0.0}_{-0.4}$
$\Lambda(1670), \Lambda(1800)$	$^{+1.5}_{-1.9}$	$^{+0.4}_{-0.4}$	$^{+0.3}_{-0.2}$	$^{+0.4}_{-0.4}$	$^{+0.1}_{-0.1}$	$^{+0.1}_{-0.1}$	$^{+0.0}_{-0.0}$	$^{+0.0}_{-0.0}$	$^{+0.0}_{-0.0}$	$^{+0.0}_{-0.1}$
$\Lambda(1690), \text{NR}(\frac{3}{2}^-)$	$^{+0.9}_{-2.2}$	$^{+1.1}_{-1.1}$	$^{+0.2}_{-2.7}$	$^{+0.2}_{-0.5}$	$^{+0.1}_{-0.1}$	$^{+0.1}_{-0.1}$	$^{+0.0}_{-0.0}$	$^{+0.0}_{-0.0}$	$^{+0.0}_{-0.1}$	$^{+0.0}_{-0.0}$
$\Lambda(1820), \Lambda(2110)$	$^{+2.4}_{-3.1}$	$^{+1.6}_{-1.6}$	$^{+0.5}_{-1.6}$	$^{+0.3}_{-0.5}$	$^{+0.2}_{-0.2}$	$^{+0.1}_{-0.1}$	$^{+0.0}_{-0.0}$	$^{+0.2}_{-0.0}$	$^{+0.0}_{-0.3}$	$^{+0.0}_{-0.2}$